Обзор arXiv: astro-ph, Jan 4-8, 2016

От Сильченко О.К.

Astro-ph: 1601.01026

Missing dark matter in dwarf galaxies?

Kyle A. Oman[1,⋆], Julio F. Navarro[1,2], Laura V. Sales[3], Azadeh Fattahi[1], Carlos S. Frenk[4], Till Sawala[4,5], Matthieu Schaller[4] and Simon D. M. White[6]

[1] *Department of Physics & Astronomy, University of Victoria, Victoria, BC, V8P 5C2, Canada*
[2] *Senior CIfAR Fellow*
[3] *Department of Physics and Astronomy, University of California at Riverside, Riversida, CA, 92521.*
[4] *Institute for Computational Cosmology, Department of Physics, University of Durham, South Road, Durham DH1 3LE, United Kingdom*
[5] *Department of Physics, University of Helsinki, Gustaf Hällströmin katu 2a, FI-00014 Helsinki, Finland*
[6] *Max Planck Institute for Astrophysics, D-85748 Garching, Germany*

Доля барионов в сравнении с космологической моделью

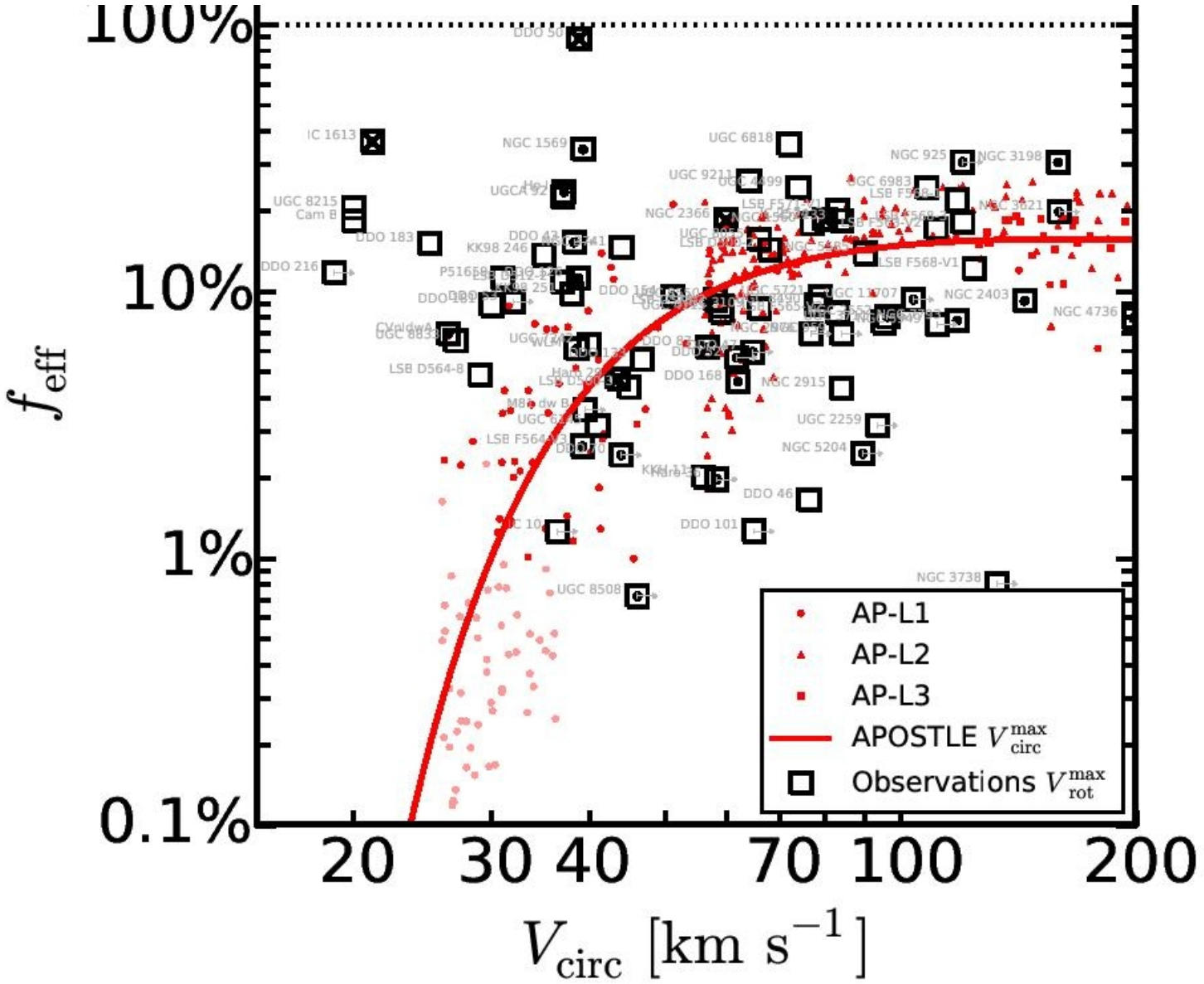

Baryonic Tully-Fisher

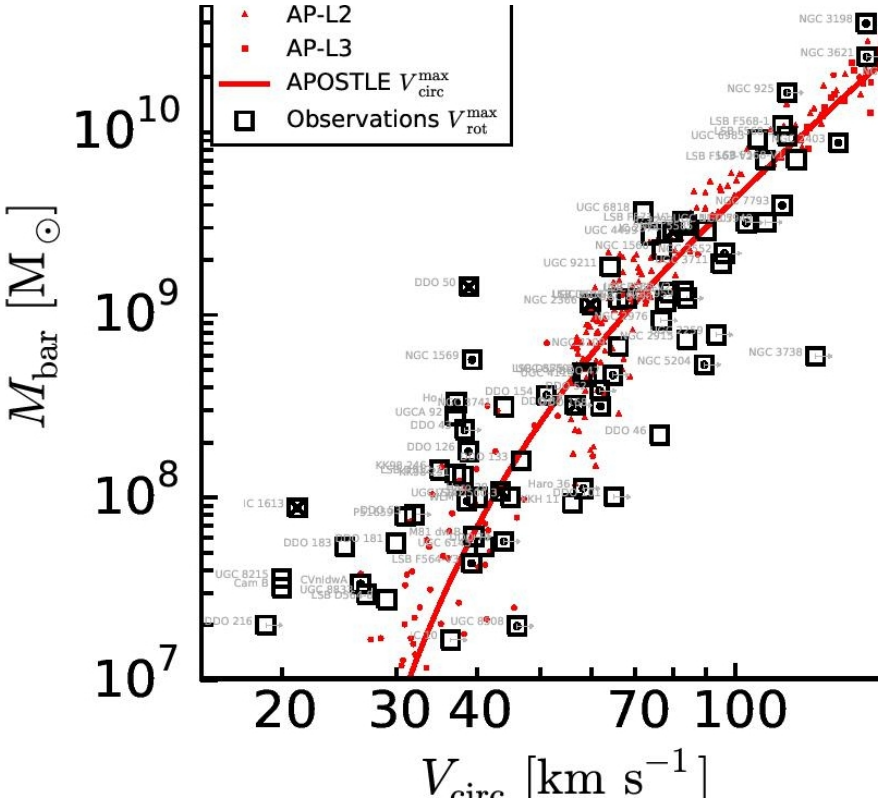

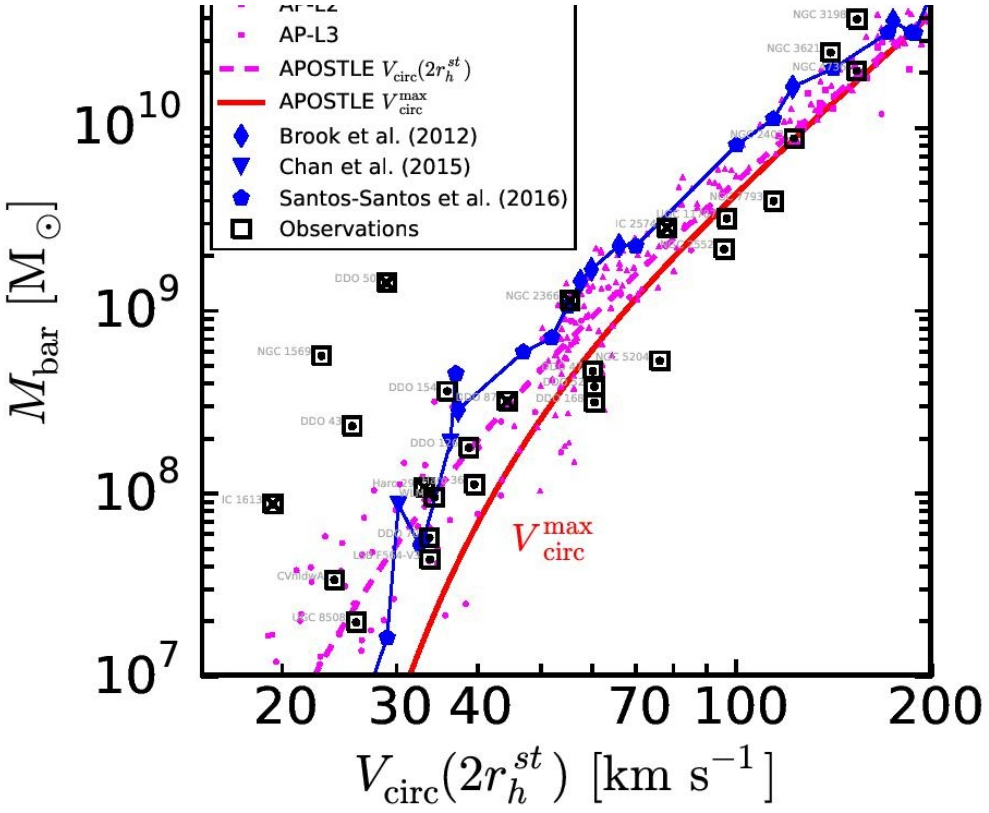

Кривые вращения в сравнении с космологической моделью

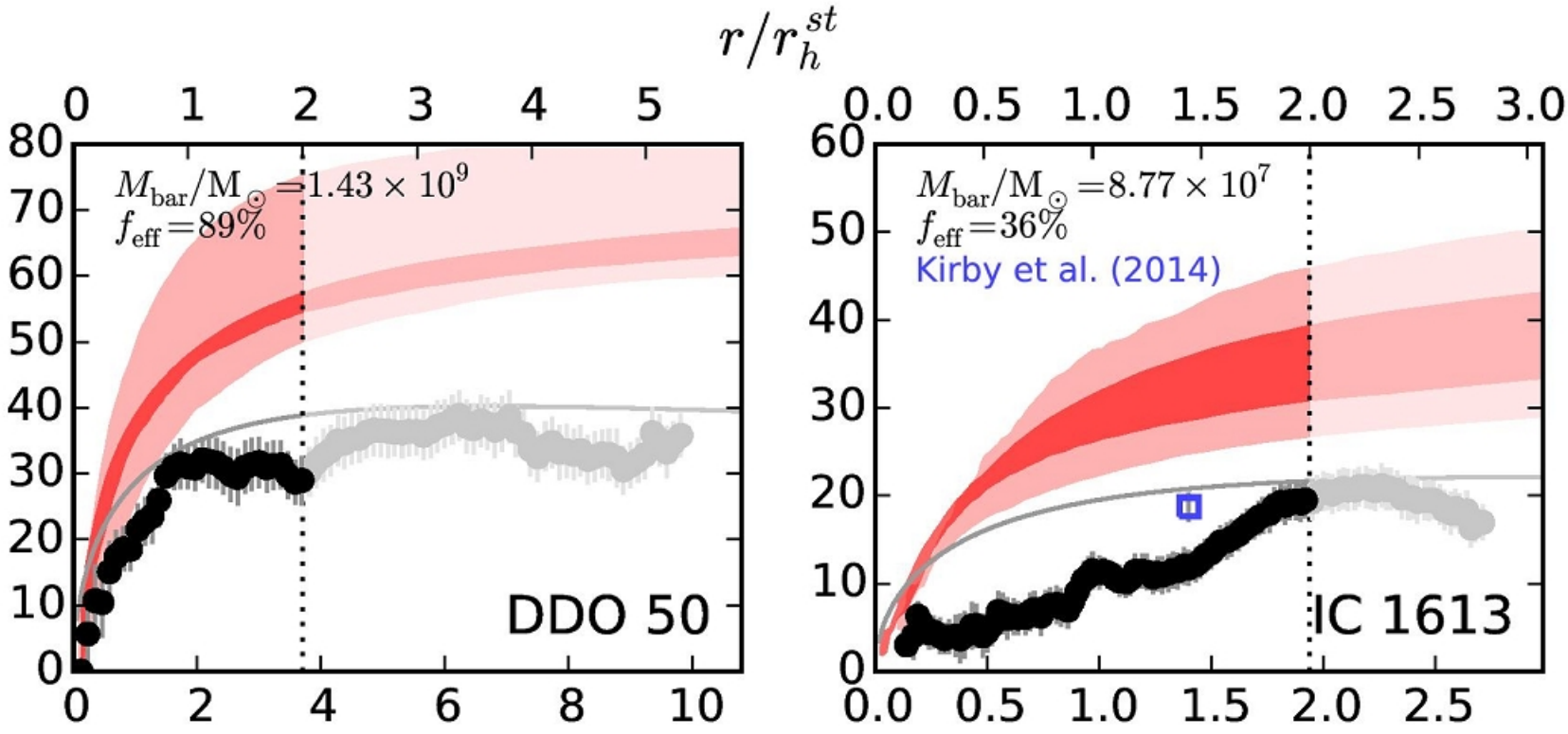

Astro-ph: 1601.01542

Shape of the oxygen abundance profiles in CALIFA face-on spiral galaxies

L. Sánchez-Menguiano[1,2], S. F. Sánchez[3], I. Pérez[2], R. García-Benito[1], B. Husemann[4], D. Mast[5,6], A. Mendoza[1], T. Ruiz-Lara[2], Y. Ascasibar[7,8], J. Bland-Hawthorn[9], O. Cavichia[10], A. I. Díaz[7,8], E. Florido[2], L. Galbany[11,12], R. M. Gónzalez Delgado[1], C. Kehrig[1], R. A. Marino[13,14], I. Márquez[1], J. Masegosa[1], J. Méndez-Abreu[15], M. Mollá[16] A. del Olmo[1], E. Pérez[1], P. Sánchez-Blázquez[7,8], V. Stanishev[17], C. J. Walcher[18], Á. R. López-Sánchez[19,20], and the CALIFA collaboration

Выборка

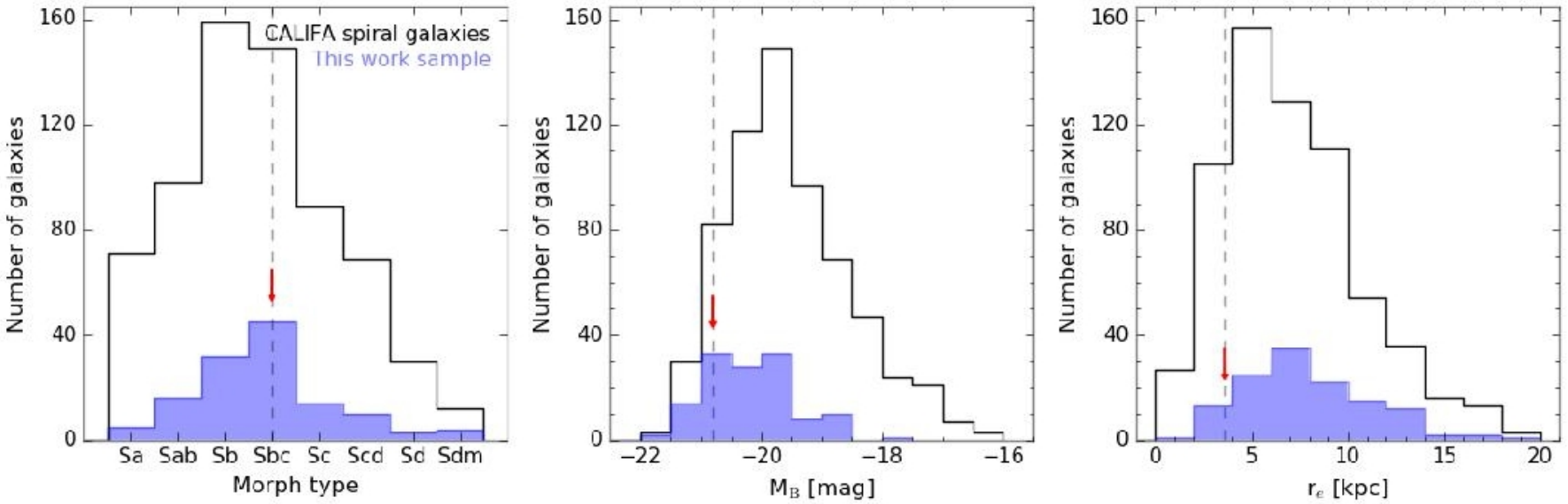
CALIFA spiral galaxies
This work sample
Number of galaxies
Morph type
Sa Sab Sb Sbc Sc Scd Sd Sdm
M_B [mag]
r_e [kpc]

Выбор калибровки металличности - неважен

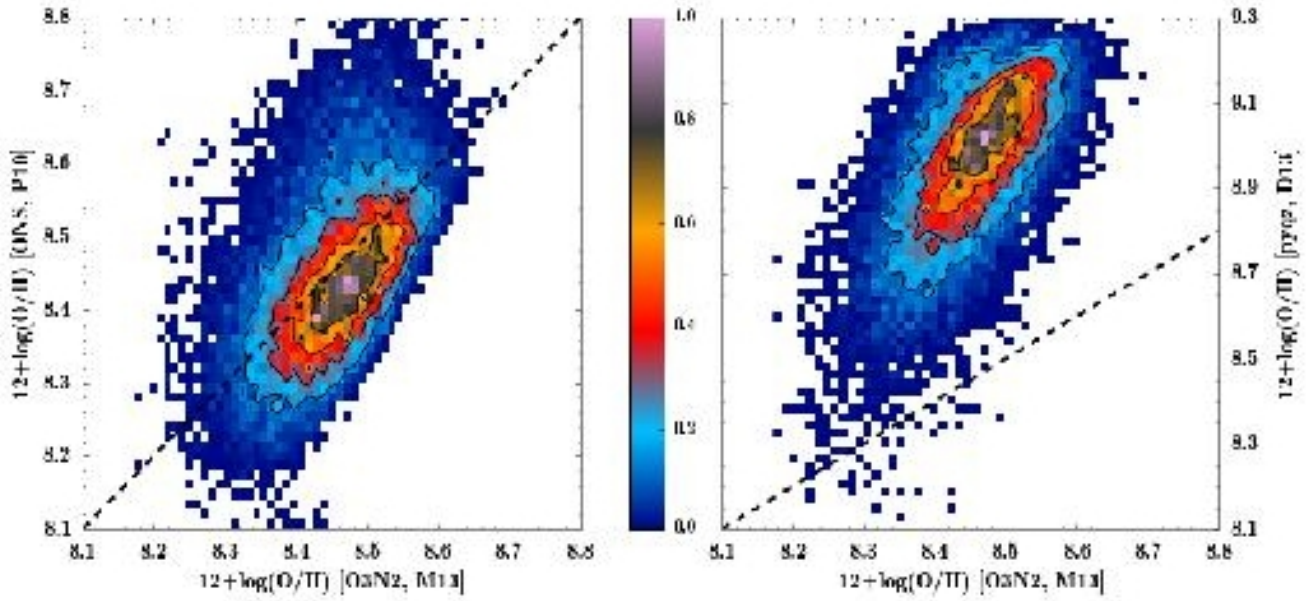

Fig. 6. Comparison of the oxygen abundance distribution derived using the calibration proposed by M13 for the O3N2 index with the distribution derived using the P10 calibration for the ONS index (left panel) and the calibration based on pyqz code (D13, right panel). The black contours show the density distribution of the SF spaxels, the outermost one including 80% of the total number of spaxels and decreasing 20% in each consecutive contour. The black dashed lines indicate the 1:1 relation between the represented calibrators.

Градиент металличности в диапазоне 0.5-2 r_e универсален

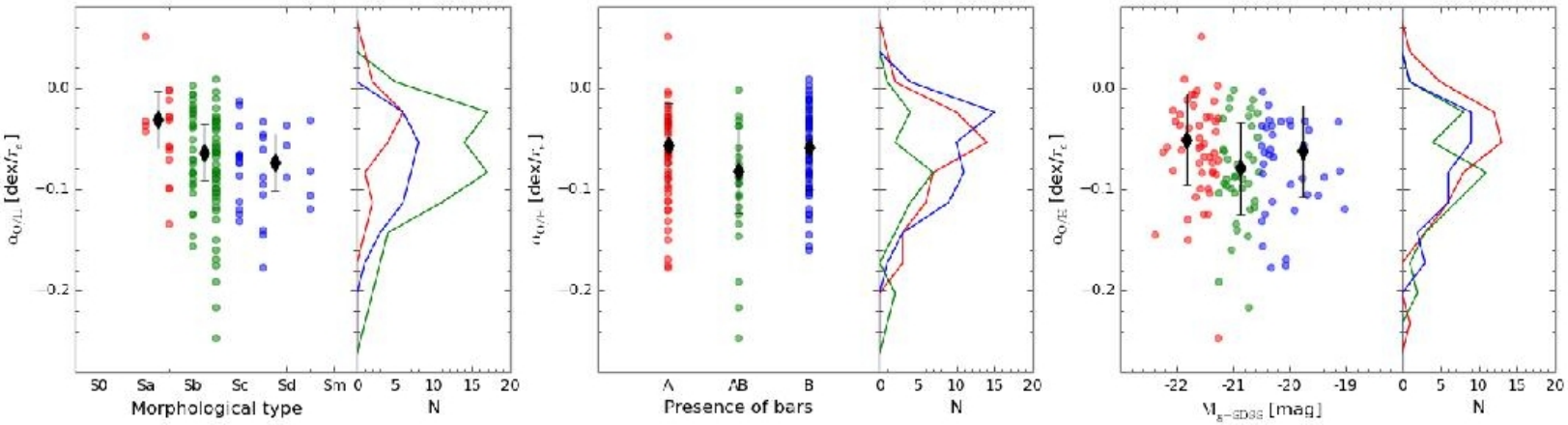

Fig. 7. Distribution of the abundance slopes as a function of the morphological type of the galaxies (left panel), depending on the presence or absence of bars (middle panel) and as a function of the g-band absolute magnitude of the galaxies (right panel). We also show the histograms for each distribution, where N is the number of galaxies and colours indicate the different classification types: (i) early spirals, Sa-Sab (red); intermediate spirals, Sb-Sbc (green); late spirals, Sc-Sm (blue) for the left panel. (ii) Clearly unbarred galaxies (red); clearly barred (blue); an intermediate stage (green) for the middle panel. (iii) Luminous galaxies, $M_{g-\mathrm{SDSS}} < -21.25$ mag (red); intermediate galaxies, $-21.25 < M_{g-\mathrm{SDSS}} < -20.5$ mag (green); faint galaxies, $M_{g-\mathrm{SDSS}} > -20.5$ mag (blue) for the right panel. Black diamonds represent the median values for the distributions, together with the standard deviation shown as error bars.

И вообще, профиль металличности универсален

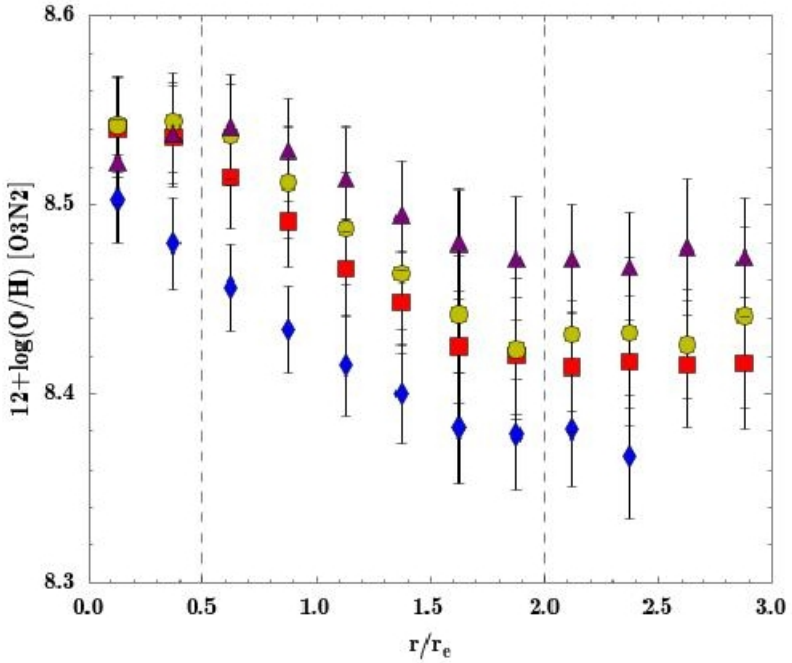

Fig. 9. Mean oxygen abundance radial profiles derived considering galaxies in four different bins according to their integrated stellar mass. The limits of the bins were chosen to ensure a similar number of elements in each bin: log ($M/M_\odot$) $\leq$ 10.2, blue diamonds; 10.2 < log ($M/M_\odot$) $\leq$ 10.5, red squares; 10.5 < log ($M/M_\odot$) $\leq$ 10.75, yellow dots; log ($M/M_\odot$) $\geq$ 10.75, purple triangles. The symbols represent the mean oxygen abundance values, with the error bars indicating the corresponding standard deviations, for bins of 0.25 r_e. Dashed vertical lines de-

Astro-ph: 1601.01589

Chemodynamic subpopulations of the Carina dwarf galaxy

G. Kordopatis,[1⋆] N. C. Amorisco,[2,3] N. W. Evans,[4] G. Gilmore,[4] S. E. Koposov[4]
[1] *Leibniz-Institut für Astrophysik Potsdam (AIP), An der Sternwarte 16, 14482 Potsdam, Germany*
[2] *Dark Cosmology Centre, Niels Bohr Institute, University of Copenhagen, Juliane Maries Vej 30, 2100 Copenhagen, Denmark*
[3] *Max Planck Institute for Astrophysics, Karl-Schwarzschild-Strasse 1, D-85740 Garching, Germany*
[4] *Institute of Astronomy, University of Cambridge, Madingley Road, Cambridge CB3 0HA, UK*

8 January 2016

ABSTRACT
We study the chemodynamical properties of the Carina dwarf spheroidal by combining an intermediate spectroscopic resolution dataset of more than 900 red giant and red clump stars, with high-precision photometry to derive the atmospheric parameters, metallicities and age

Выборка звезд-гигантов и «красный сгусток»

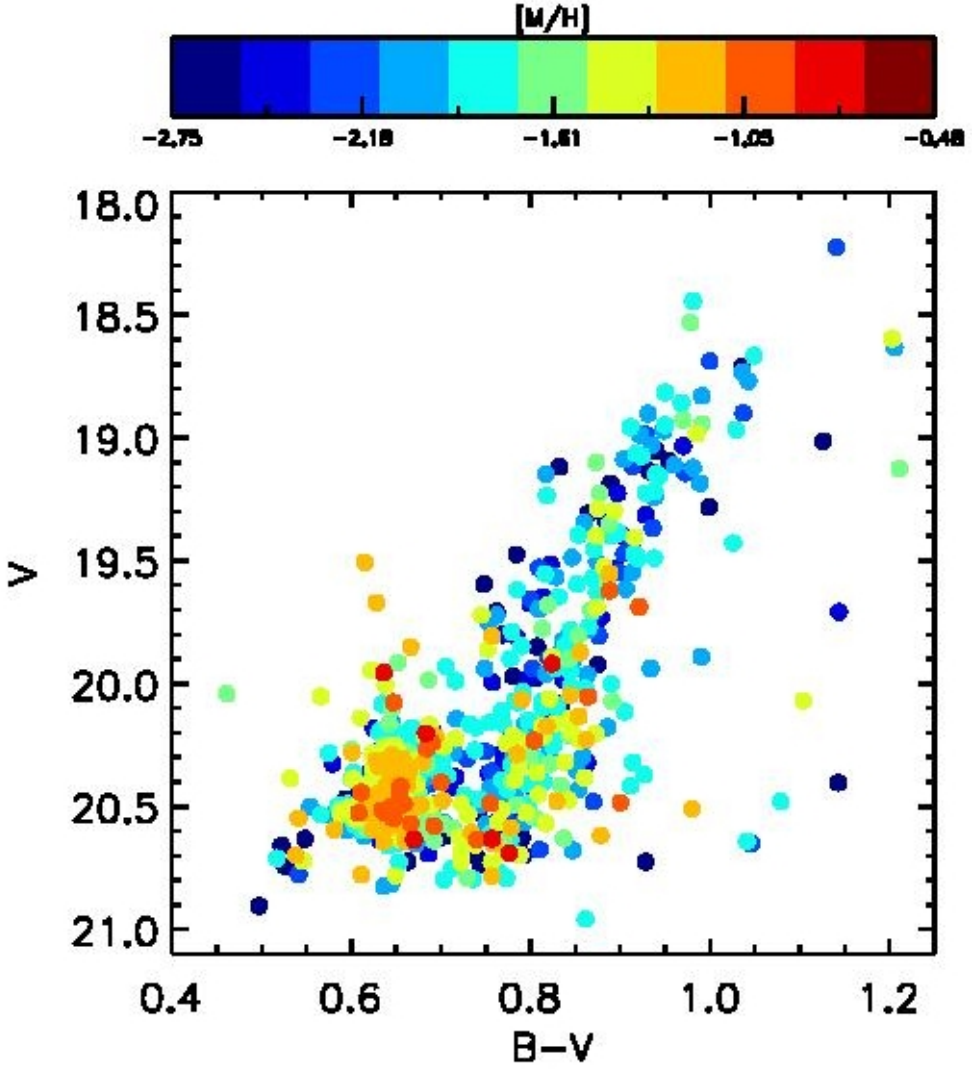

История звездообразования

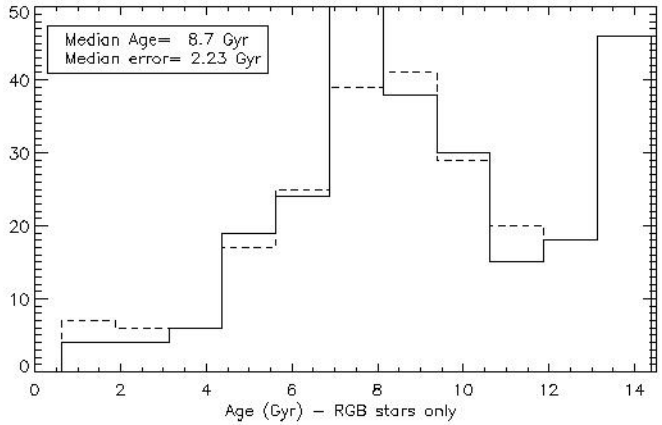

Figure 6. Age distribution of the RGB stars of Carina. The dotted (plain) line corresponds to age estimations with (without) taking into account the information on the effective temperature and gravity.

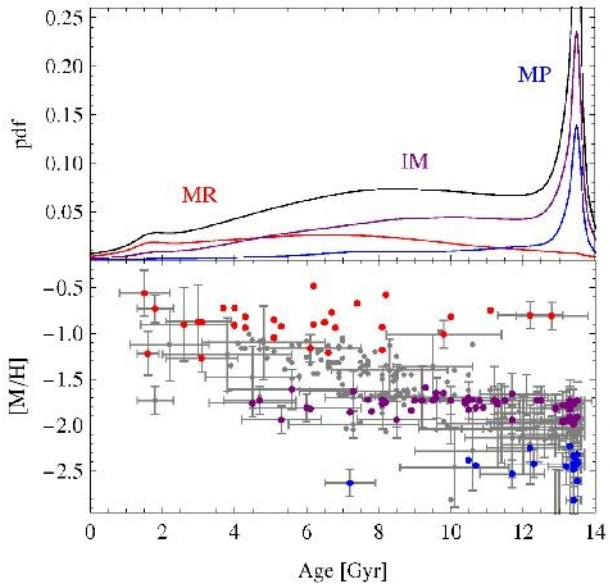

Figure 9. Subpopulations and ages. Upper panel: the probability distribution for the age of the three distinct chemo-dynamical subpopulations in Carina (metal rich in red, intermediate in purple, metal poor in blue, total in black). Lower panel: the age-metallicity diagram for the RGB stars in the spectroscopic sample; error bars are shown only for stars with a precise age estimate ($\delta_{\rm age} \leqslant 1.5$ Gyr); colored points identify high-probability members (probability of being a member larger than 75 percent) for each chemo-dynamical subpopulation.

Три населения – выбраны по металличности и по динамике

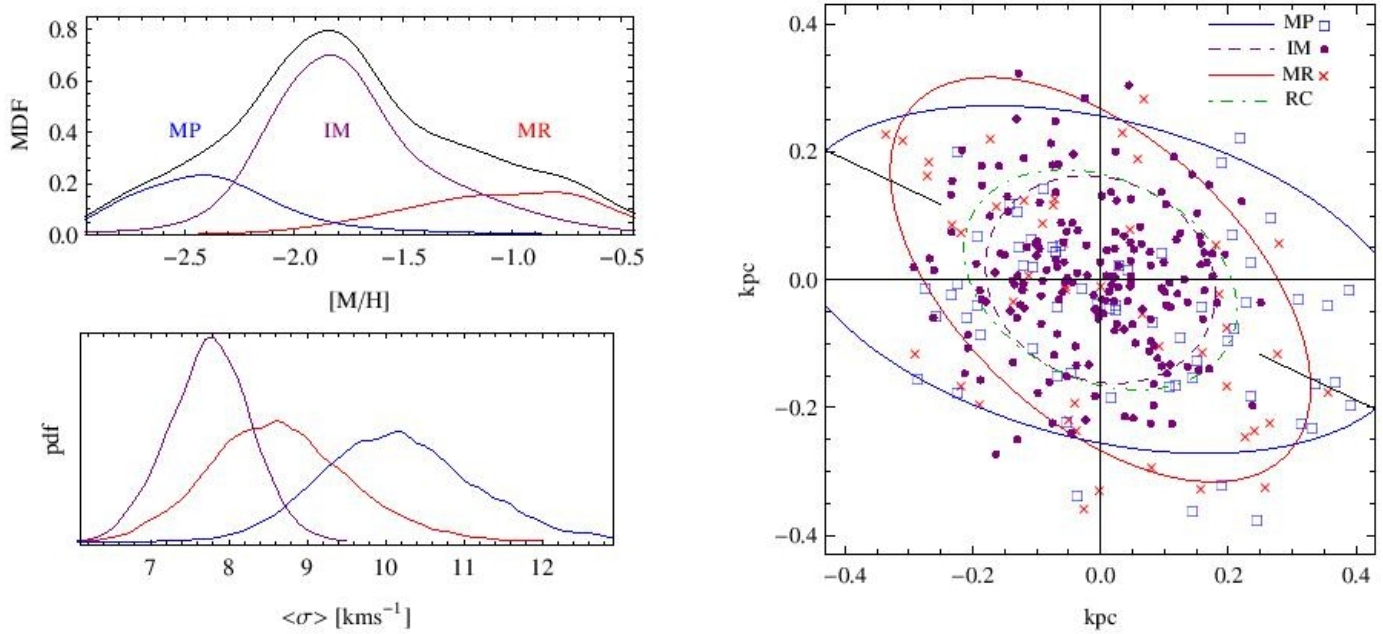

Figure 7. Three distinct subpopulations. Left upper panel: metallicity distribution function decomposed in three populations. Black: the MDF of the entire RGB sample. Blue, purple and red, respectively the contributions of metal-poor, intermediate-metallicity and metal-rich populations to the global RGB MDF.

Самый поздний компонент – разогрет динамически?

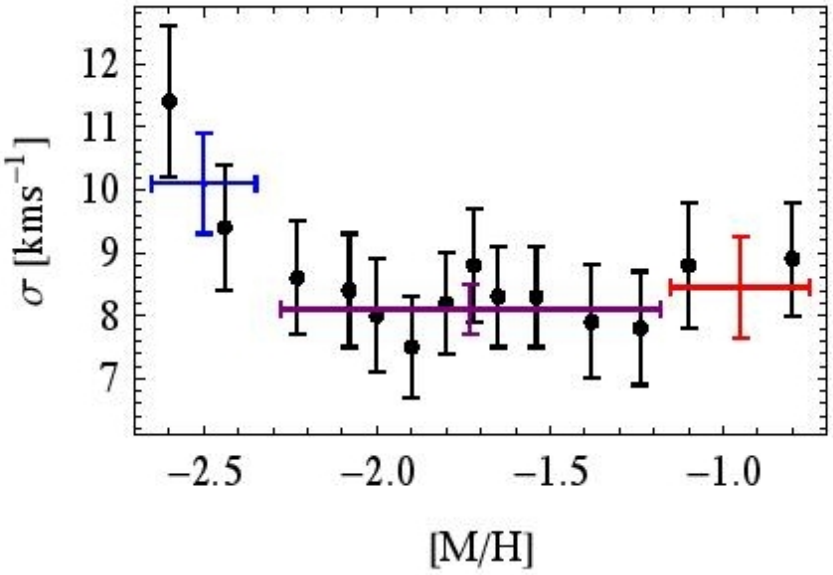

Figure 8. Projected velocity dispersion versus metallicity, obtained by simply binning the spectroscopic data for the RGBs. Black points are obtained using subsets of 50 RGBs each (successive bins shift by 25 stars at a time, so that not all data points are independent). All measurements are obtained through a maximum likelihood method, and the vertical error bars show 1σ uncertainties. The wider and coloured error bars group RGB stars into wider bins, and are fully independent from each other (respectively, the three bins contain 75, 250, 75 RGBs).